JACS
JOURNAL OF THE AMERICAN CHEMICAL SOCIETY
Communication
pubs.acs.org/JACS

Self-Assembly of Highly Ordered Peptide Amphiphile Metalloporphyrin Arrays

H. Christopher Fry,*[,†] Jamie M. Garcia,[‡] Matthew J. Medina,[‡] Ulises M. Ricoy,[‡] David J. Gosztola,[†] Maxim P. Nikiforov,[†] Liam C. Palmer,[⊥] and Samuel I. Stupp[§,∥,⊥]

[†]Center for Nanoscale Materials, Argonne National Laboratory, Argonne, Illinois 60439, United States

[‡]Northern New Mexico College, Española, New Mexico 87532, United States

[§]Department of Material Science and Engineering and [⊥]Department of Chemistry, Northwestern University, Evanston, Illinois 60208 United States

[∥]Institute for BioNanotechnology in Medicine and Department of Medicine, Northwestern University, Chicago, Illinois 60611, United States

Supporting Information

ABSTRACT: Long fibers assembled from peptide amphiphiles capable of binding the metalloporphyrin zinc protoporphyrin IX ((PPIX)Zn) have been synthesized. Rational peptide design was employed to generate a peptide, c16-AHL_3K_3-CO_2H, capable of forming a β-sheet structure that propagates into larger fibrous structures. A porphyrin-binding site, a single histidine, was engineered into the peptide sequence in order to bind (PPIX)Zn to provide photophysical functionality. The resulting system indicates control from the molecular level to the macromolecular level with a high order of porphyrin organization. UV/visible and circular dichroism spectroscopies were employed to detail molecular organization, whereas electron microscopy and atomic force microscopy aided in macromolecular characterization. Preliminary picosecond transient absorption data are also reported. Reduced hemin, (PPIX)Fe^{II}, was also employed to highlight the material's versatility and tunability.

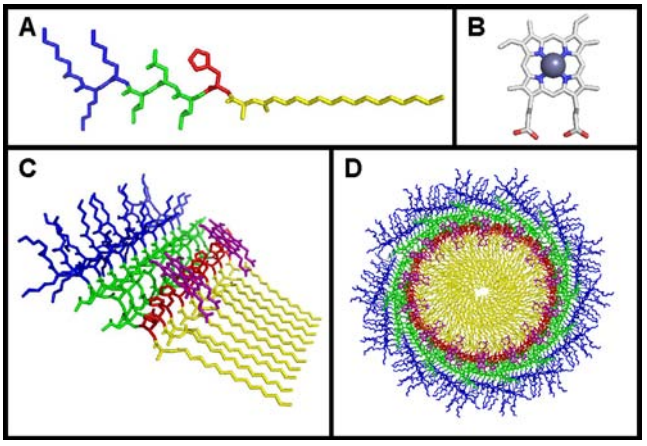

Figure 1. (A) Peptide design: c16-AHL_3K_3-CO_2H lysine (blue), leucine (green), histidine (red), alanine and c16 (yellow). (B) (PPIX)Zn. (C) β-Sheet organization with (PPIX)Zn (purple). (D) Cross section of self-assembled fiber.

Nature utilizes macrocyclic molecules in organized arrays of proteins to function as electron-transfer sites (cytochrome bc1),[1,2] catalytic reaction centers (cytochrome p450, cytochrome *c* oxidase),[3,4] and light-harvesting complexes (LHCs; photosystems I and II).[5] In particular, the LHC[6,7] from purple bacteria highlights one of nature's most fascinating capabilities, the self-assembly of basic building blocks, peptides and chlorophyll, into a well-ordered and well-structured functional material. By organizing a multitude of chromophores in a controlled manner, nature has devised a means of collecting sunlight and utilizing that sunlight to catalyze the synthesis of useful fuel. Here, we employ peptide amphiphiles as the structural architecture to guide the formation of fibrous assemblies while ordering metalloporphyrins in a well-organized manner.

Peptide-directed self-assembly is an ever-expanding tool in the development of useful nanomaterials.[8] Peptide amphiphiles[9,10] that can self-assemble into high-aspect-ratio nanofibers have recently been employed in a wide array of functions including directed cell proliferation,[11,12] nanoparticle organization,[13] and bone regeneration[9] to name a few. Based on the peptide amphiphiles' versatility through rational design, we explore here their potential as scaffolds for "light-harvesting fibers". To date, empirical and computationally derived coiled-coils dominate the literature regarding binding of metalloporphyrins to designed peptide frameworks.[14−27] However, these tetra-α-helical bundles were designed to yield water-soluble monomeric units capable of binding 1−4 chromophores. To generate a useful material, the long-range ordering of exogenous chromophores, like porphyrins, is necessary.[28] The design presented herein consists of a standard amphiphilic motif (Figure 1): a polar head, to which we have assigned three lysine residues, and a nonpolar, aliphatic tail, palmitic acid. Three leucine residues were employed to enhance structural organization using well-documented β-sheet conformers.[29−31] Leucine possesses moderate β-sheet propensity and was strategically chosen to provide a handle for control over the rate of fiber formation. A metalloporphyrin binding site of a single histidine was chosen, as it is the predominant axial ligand

Received: May 14, 2012
Published: August 23, 2012

dx.doi.org/10.1021/ja304674d | *J. Am. Chem. Soc.* 2012, 134, 14646−14649

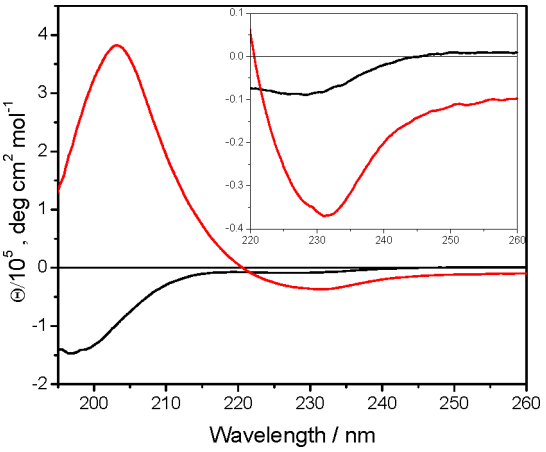

Figure 2. CD spectra of 500 μM c16-AHL$_3$K$_3$-CO$_2$H in water (black) and 125 mM NH$_4$OH (red). Inset: expanded view of the minima representing the β-sheet signal.

for many metalloporphyrin cofactors found in naturally occurring proteins.[1−7] Finally, to provide additional space for the chromophore to bind, a single alanine was introduced as a spacer between the functional binding group and the aliphatic tail. The final sequence, c16-AHL$_3$K$_3$-CO$_2$H, yielded the ideal porphyrin-binding peptide amphiphile. Once assembled, the peptide fibers would have a diameter between 6.9 (fully interdigitated alkyl tail) and 9.0 nm (fully extended peptide) (Figure S1).

The peptide was synthesized using standard solid-phase Fmoc-based chemistry and purified by RP-HPLC (Figure S2). Dissolution of the peptide amphiphile in water at a concentration of 1 wt%, 8.4 mM, results in a fluid solution. Upon addition of ammonium hydroxide (final NH$_4$OH concentration, 125 mM), the solution immediately becomes viscous and ultimately forms a self-supporting gel (Figure S3). CD spectroscopy indicates that in water a sample of c16-AHL$_3$K$_3$-CO$_2$H (500 μM) yields no observable structure, even when the sample is aged for days (Figure 2). Addition of NH$_4$OH yields a twisted or aggregated β-sheet conformation, as indicated by the red-shifted 218 nm signature band of a typical β-sheet.[32,33] Time-dependent measurements on samples at various concentrations of c16-AHL$_3$K$_3$-CO$_2$H followed by addition of 125 mM NH$_4$OH indicate immediate formation of a β-sheet followed by additional twisting/aggregation of a larger structure (218→231 nm) over 30 min (Figures S4−S6). This slow transition allows for the timely incorporation of an exogenous substrate, such as a metalloporphyrin chromophore.

Zinc protoporphyrin IX ((PPIX)Zn, 50 μM) was added to a solution of c16-AHL$_3$K$_3$-CO$_2$H (500 μM in 125 mM NH$_4$OH) that had been aged for 1 h. UV/vis spectroscopy indicates histidyl axial binding of the chromophore, as the B-band (λ_{max} = 431 nm) and Q-bands (λ_{max} = 552, 589 nm) are red-shifted from the unbound (PPIX)Zn in 125 mM NH$_4$OH (B-band, λ_{max} = 412 nm; Q-bands, λ_{max} = 550, 586 nm; Figure S7). Interestingly, circular dichroism indicates a strong signal in the visible region with a negative Cotton effect (λ_{min}) at 425 nm and positive Cotton effect (λ_{max}) at 433 nm (Figure S7). Such a strong signal is indicative of exciton coupling between well-ordered neighboring chromophores.[25,34,35] No observable signal was obtained in the absence of peptide. A temporal component has also been noted in the sample preparation that directly coincides with β-sheet formation. Addition of the chromophore into the

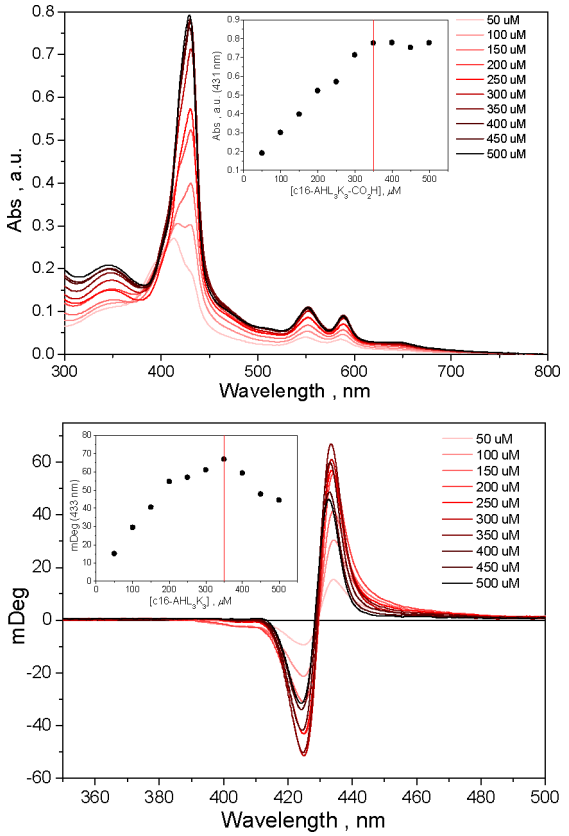

Figure 3. Titration of c16-AHL$_3$K$_3$-CO$_2$H into (PPIX)Zn, monitored by UV/vis and CD spectroscopy. (Top) Absorption and (bottom) CD spectra of 50 μM (PPIX)Zn in 125 mM NH$_4$OH with 50−500 μM c16-AHL$_3$K$_3$-CO$_2$H. Insets: dependence of (PPIX)Zn B-band absorption, 431 nm (top), and positive Cotton band, 433 nm (bottom), on c16-AHL$_3$K$_3$-CO$_2$H concentration.

material solution immediately after adding NH$_4$OH and after 2 h incubation results in inefficient binding (UV/vis signal decrease) and ordering (CD signal decrease) of (PPIX)Zn, suggesting a moderately narrow window for cofactor addition at these concentrations. Before addition of base, the structure is not formed, and after 2 h, fiber bundling becomes extensive. Between those times, we suggest there is an optimal window in which accessible water channels are available for the (PPIX)Zn molecule to migrate toward the hydrophobic core and bind to the available histidine moiety.[36,37]

To determine the stoichiometry, or porphyrin loading capacity, of the peptide material, titrations were performed holding the chromophore constant at 50 μM while varying the peptide concentration from 50 to 500 μM. Based on the model (Figure S1), we expected roughly a 1:4 metalloporphyrin/peptide stoichiometry. By monitoring the B-band (431 nm) in the absorption spectrum which corresponds to the axially bound cofactor (Figure 3), we found a 1:6 stoichiometry. CD spectra elicit a unique insight into the porphyrin organization. The largest observed signal in the CD titration was observed at a 1:6 stoichiometry, consistent with that found for the UV/vis titration (Figure 3). This suggests that the porphyrin is tightly packed, with a small interchromophore distance at a fixed dihedral angle in the assembled peptide material at this stoichiometry.[34] At a 1:10 stoichiometry, this signal was decreased by nearly a factor of 2, consistent with an increase in chromophore−chromophore distance. We did not observe the expected 1:4 stoichiometry,

dx.doi.org/10.1021/ja304674d | J. Am. Chem. Soc. 2012, 134, 14646−14649

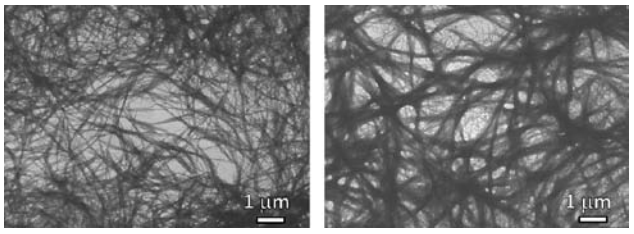

Figure 4. SEM images of fibers formed from addition of 125 mM NH_4OH to c16-AHL_3K_3-CO_2H, without (left) and with (right) (PPIX)Zn.

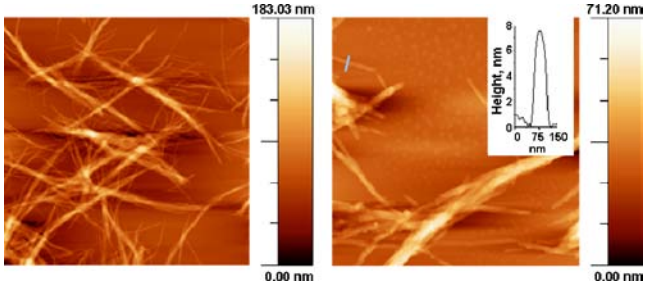

Figure 5. AFM images of fibers formed from addition of 125 mM NH_4OH to c16-AHL_3K_3-CO_2H with (PPIX)Zn. Left, 10 × 10 μm; right image, 2.5 × 2.5 μm; inset, height profile of a single fiber.

most likely due to potential steric interactions between the bulky side chains of neighboring (PPIX)Zn molecules. In addition, the model (Figure S1) assumes a very flat and planar β-sheet, whereas twisting of the structure could induce a change in the binding site, lending itself to the observed 1:6 stoichiometry.

The supramolecular assembly of the material was analyzed by SEM with a transmission electron detector (TED). In water, irregular spherical or disk-like structures are observed (Figure S8). Upon addition of NH_4OH, we observe bundling fibers (Figure 4). In conjunction with the observed CD data, it can be concluded that β-sheet formation is a precursor to the formation of the bundled fibers. The degree of bundling is somewhat controlled (i.e., number of fibers per bundle) by modifying the concentration at which the fibers are formed (Figure S9). As the concentration increases, bundling increases. The addition of (PPIX)Zn does not have any influence over the sample morphology (Figure 4). The fibers were noted to be micrometers in length and significantly entangled. AFM was performed to analyze the height dimensions of the fibers (Figure 5). Interestingly, we observed single, double, triple, etc. fibers. The single fibers exhibited 7−9 nm height, consistent with the molecular model of the peptide (6.8−8.9 nm).

To probe the photophysical properties of the long order arrangement of (PPIX)Zn, femtosecond transient absorption spectroscopy was employed.[38] Upon excitation at 430 nm, the first sample, (PPIX)Zn in 50 μM DMSO under an inert atmosphere, was found to have a lifetime much greater than the upper limits of our instrumental setup (Figure S10, top). The difference spectra in the microsecond time regime indicated formation of the expected triplet excited state. The kinetic profile yielded a plateau extended to 5 μs. Typically, the zinc porphyrin triplet excited state exhibits a millisecond lifetime.[39] The second sample, 50 μM (PPIX)Zn in 125 mM NH_4OH, is not stable for long times and tends to aggregate under these conditions, exhibiting significant exciton annihilation contributions (Figure S10, bottom). Interestingly, the third sample, (PPIX)Zn:c16-AHL_3K_3-CO_2H complex (1:10 porphyrin/peptide to ensure

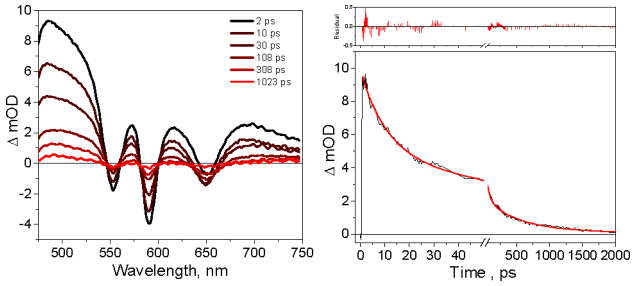

Figure 6. Transient absorption (λ_{ex} = 430 nm) difference spectra at selected delay times (left) and kinetics measured at 490 nm (right), raw data (black line), and triexponential kinetic fit, τ_1 = 10.3 ps, τ_2 = 56.6 ps, and τ_3 = 570 ps (red line) of (PPIX)Zn:c16-AHL_3K_3-CO_2H (1:10) in 125 mM NH_4OH. Residual graph represents the difference between the kinetic fit and the data.

complete cofactor binding), exhibits no observable triplet excited state in the microsecond time regime (Figure 6). The observed multicomponent time processes on the picosecond time scale are consistent with singlet exciton annihilation interactions between neighboring excited chromophores.[26,40−42]

To better understand the chromophore organization, a second peptide was synthesized, c16-AH*A*L_3K_3-CO_2H, that incorporated an extra alanine between the porphyrin-binding histidine and the β-sheet structural region of the peptide. We found that the peptide formed standard β-sheets (218 nm; Figure S11) and did indeed bind (PPIX)Zn, but strong exciton coupling was not observed in the visible region of the CD spectrum (Figure S12). The morphology of the self-assembled peptide in a basic solution without and with (PPIX)Zn was the same as that of the parent peptide. However, it was noticed that, over time (1 day), a 1 wt% solution of c16-AH*A*L_3K_3-CO_2H in water formed a viscous solution. SEM (TED) indicated self-assembly of fibers and sheets in the absence of base (Figure S13). This lack of control over the pH-triggered assembly may suggest the additional alanine contributes to a stronger β-sheet-forming peptide, but a less rigid porphyrin-binding pocket results due to the poor space-filling of the alanine residue. Due to the seemingly minor addition to the peptide sequence, the alanine residue provides insight into next-generation designs of peptide amphiphiles capable of binding metalloporphyrins.

Finally, the modularity of the material was tested. Hemin is simply protoporphyrin IX with a ferric (Fe^{3+}) ion as the metal center. It is found in all living mammals, serving as a redox-active center with applications in electron transfer as well as oxygen binding and activation. The ferric center prefers six-coordinate geometry, while the ferrous (Fe^{2+}) ion prefers five-coordinate geometry, similar to that of zinc. We were able to confirm binding in the ferrous state to the peptide by the red-shifted UV/vis data (B-band, λ_{max} = 426 nm; Q-bands, λ_{max} = 527, 559 nm) and exciton interactions of neighboring chromophores by CD spectroscopy with a negative Cotton effect (λ_{min}) at 421 nm and positive Cotton effect (λ_{max}) at 434 nm (Figure S14). The peptide, c16-AHL_3K_3-CO_2H, successfully incorporates both ferrous and (PPIX)Zn cofactors. Therefore, the material character can be tuned (i.e., from a light-harvesting fiber with (PPIX)Zn to an oxygen-activating fiber with reduced hemin) simply by exchanging cofactors that require a single axial histidine ligand.

In comparison to other metalloporphyrin-binding peptide systems, peptide amphiphiles offer several advantages: (1) The long-aspect-ratio fibers housing metalloporphyrins provide a

dx.doi.org/10.1021/ja304674d | J. Am. Chem. Soc. 2012, 134, 14646−14649

readily available platform for employment as a molecular wire, as opposed to other metalloporphyrin-binding peptides that would require some element of post-processing, i.e., surface immobilization. (2) The fiber itself provides an overabundance of metalloporphyrin-binding sites, allowing the material to be tuned simply by loading the material to its 1:6 chromophore/peptide maximum loading capacity or well below that value to obtain the desired photophysical/electronic characteristics. (3) Finally, the single histidine available for binding allows for material tunability simply by incorporating the metalloporphyrin with the desired physical property, in this case (PPIX)Zn for photoexcitation or hemin for oxygen activation.

In conclusion, we have exhibited excellent control over porphyin organization from the molecular to the macromolecular scales by using a simple peptide amphiphile design. Upon addition of base, β-sheet formation propagates the formation of larger fibrous structures capable of binding and encapsulating a photoactive chromophore, (PPIX)Zn, as well as an oxygen-activating chromophore, reduced hemin. The assembly indicates strong exciton interactions between neighboring chromophores, suggesting a tight packing and close proximity. Photophysical measurements indicate a definite influence of the peptide on the electronic interactions of the chromophore. Further studies will focus on obtaining physical measurements of the fibrous material and varying the peptide sequence and cofactor to produce a more stable peptide-based photovoltaic material.

■ ASSOCIATED CONTENT

Supporting Information

Experimental details; molecular modeling; CD and absorption spectroscopy; and electron microscopy. This material is available free of charge via the Internet at http://pubs.acs.org.

■ AUTHOR INFORMATION

Corresponding Author

hfry@anl.gov

Notes

The authors declare no competing financial interest.

■ ACKNOWLEDGMENTS

The authors thank Tijana Rajh for helpful discussions. This work was performed, in part, at the Center for Nanoscale Materials, a U.S. Department of Energy, Office of Science, Office of Basic Energy Sciences User Facility under Contract No. DE-AC02-06CH11357. U.M.R., J.M.G., and M.J.M. were supported by the Department of Energy, Office of Science, Workforce Development for Teachers and Scientists and the Division of Educational Programs at ANL. L.C.P. and S.I.S. were supported by U.S. Department of Energy, US DOE-BES, under Contract No. DE-FG02- 00ER45810.

■ REFERENCES

(1) Lange, C.; Hunte, C. *Proc. Natl. Acad. Sci. U.S.A.* **2002**, *99*, 2800.
(2) Zhang, Z. L.; Huang, L. S.; Shulmeister, V. M.; Chi, Y. I.; Kim, K. K.; Hung, L. W.; Crofts, A. R.; Berry, E. A.; Kim, S. H. *Nature* **1998**, *392*, 677.
(3) Meunier, B.; de Visser, S. P.; Shaik, S. *Chem. Rev.* **2004**, *104*, 3947.
(4) FergusonMiller, S.; Babcock, G. T. *Chem. Rev.* **1996**, *96*, 2889.
(5) Ferreira, K. N.; Iverson, T. M.; Maghlaoui, K.; Barber, J.; Iwata, S. *Science* **2004**, *303*, 1831.
(6) Koepke, J.; Hu, X. C.; Muenke, C.; Schulten, K.; Michel, H. *Structure* **1996**, *4*, 581.
(7) Scholes, G. D.; Fleming, G. R. *J. Phys. Chem. B* **2000**, *104*, 1854.
(8) Ulijn, R. V.; Smith, A. M. *Chem. Soc. Rev.* **2008**, *37*, 664.
(9) Hartgerink, J. D.; Beniash, E.; Stupp, S. I. *Science* **2001**, *294*, 1684.
(10) Matson, J. B.; Stupp, S. I. *Chem. Commun.* **2012**, *48*, 26.
(11) Silva, G. A.; Czeisler, C.; Niece, K. L.; Beniash, E.; Harrington, D. A.; Kessler, J. A.; Stupp, S. I. *Science* **2004**, *303*, 1352.
(12) Tysseling-Mattiace, V. M.; Sahni, V.; Niece, K. L.; Birch, D.; Czeisler, C.; Fehlings, M. G.; Stupp, S. I.; Kessler, J. A. *J. Neurosci.* **2008**, *28*, 3814.
(13) Chen, C. L.; Zhang, P. J.; Rosi, N. L. *J. Am. Chem. Soc.* **2008**, *130*, 13555.
(14) Cochran, F. V.; Wu, S. P.; Wang, W.; Nanda, V.; Saven, J. G.; Therien, M. J.; DeGrado, W. F. *J. Am. Chem. Soc.* **2005**, *127*, 1346.
(15) Bender, G. M.; Lehmann, A.; Zou, H.; Cheng, H.; Fry, H. C.; Engel, D.; Therien, M. J.; Blasie, J. K.; Roder, H.; Saven, J. G.; DeGrado, W. F. *J. Am. Chem. Soc.* **2007**, *129*, 10732.
(16) McAllister, K. A.; Zou, H.; Cochran, F. V.; Bender, G. M.; Senes, A.; Fry, H. C.; Nanda, V.; Keenan, P. A.; Lear, J. D.; Saven, J. G.; Therien, M. J.; Blasie, J. K.; DeGrado, W. F. *J. Am. Chem. Soc.* **2008**, *130*, 11921.
(17) Fry, H. C.; Lehmann, A.; Saven, J. G.; DeGrado, W. F.; Therien, M. J. *J. Am. Chem. Soc.* **2010**, *132*, 3997.
(18) Korendovych, I. V.; Senes, A.; Kim, Y. H.; Lear, J. D.; Fry, H. C.; Therien, M. J.; Blasie, J. K.; Walker, F. A.; DeGrado, W. F. *J. Am. Chem. Soc.* **2010**, *132*, 15516.
(19) Robertson, D. E.; Farid, R. S.; Moser, C. C.; Urbauer, J. L.; Mulholland, S. E.; Pidikiti, R.; Lear, J. D.; Wand, A. J.; Degrado, W. F.; Dutton, P. L. *Nature* **1994**, *368*, 425.
(20) Gibney, B. R.; Rabanal, F.; Skalicky, J. J.; Wand, A. J.; Dutton, P. L. *J. Am. Chem. Soc.* **1997**, *119*, 2323.
(21) Gibney, B. R.; Dutton, P. L. *Protein Sci.* **1999**, *8*, 1888.
(22) Shifman, J. M.; Gibney, B. R.; Sharp, R. E.; Dutton, P. L. *Biochemistry* **2000**, *39*, 14813.
(23) Chen, X. X.; Discher, B. M.; Pilloud, D. L.; Gibney, B. R.; Moser, C. C.; Dutton, P. L. *J. Phys. Chem. B.* **2002**, *106*, 617.
(24) Koder, R. L.; Anderson, J. L. R.; Solomon, L. A.; Reddy, K. S.; Moser, C. C.; Dutton, P. L. *Nature* **2009**, *458*, 305.
(25) Kuciauskas, D.; Caputo, G. A. *J. Phys. Chem. B.* **2009**, *113*, 14439.
(26) Kuciauskas, D.; Riskis, J.; Caputo, G. A.; Gulbinas, V. *J. Phys. Chem. B.* **2010**, *114*, 16029.
(27) Reedy, C. J.; Gibney, B. R. *Chem. Rev.* **2004**, *104*, 617.
(28) Pepe-Mooney, B. J.; Kokona, B.; Fairman, R. *Biomacromolecules* **2011**, *12*, 4196.
(29) Kim, C. W. A.; Berg, J. M. *Nature* **1993**, *362*, 267.
(30) Minor, D. L.; Kim, P. S. *Nature* **1994**, *367*, 660.
(31) Smith, C. K.; Withka, J. M.; Regan, L. *Biochemistry* **1994**, *33*, 5510.
(32) Pashuck, E. T.; Cui, H. G.; Stupp, S. I. *J. Am. Chem. Soc.* **2010**, *132*, 6041.
(33) Manning, M. C.; Illangasekare, M.; Woody, R. W. *Biophys. Chem.* **1988**, *31*, 77.
(34) Guryanov, I.; Moretto, A.; Campestrini, S.; Broxterman, Q. B.; Kaptein, B.; Peggion, C.; Formaggio, F.; Toniolo, C. *Biopolymers* **2006**, *82*, 482.
(35) Pescitelli, G.; Gabriel, S.; Wang, Y. K.; Fleischhauer, J.; Woody, R. W.; Berova, N. *J. Am. Chem. Soc.* **2003**, *125*, 7613.
(36) Tovar, J. D.; Claussen, R. C.; Stupp, S. I. *J. Am. Chem. Soc.* **2005**, *127*, 7337.
(37) Lee, O. S.; Stupp, S. I.; Schatz, G. C. *J. Am. Chem. Soc.* **2011**, *133*, 3677.
(38) Pelton, M.; Sader, J. E.; Burgin, J.; Liu, M. Z.; Guyot-Sionnest, P.; Gosztola, D. *Nat. Nanotechnol.* **2009**, *4*, 492.
(39) Kim, J. E.; Pribisko, M. A.; Gray, H. B.; Winkler, J. R. *Inorg. Chem.* **2004**, *43*, 7953.
(40) Aratani, N.; Kim, D.; Osuka, A. *Acc. Chem. Res.* **2009**, *42*, 1922.
(41) Hwang, I. W.; Park, M.; Ahn, T. K.; Yoon, Z. S.; Ko, D. M.; Kim, D.; Ito, F.; Ishibashi, Y.; Khan, S. R.; Nagasawa, Y.; Miyasaka, H.; Keda, C.; Takahashi, R.; Ogawa, K.; Satake, A.; Kobuke, Y. *Chem. Eur. J.* **2005**, *11*, 3753.
(42) Hwang, I. W.; Kamada, T.; Ahn, T. K.; Ko, D. M.; Nakamura, T.; Tsuda, A.; Osuka, A.; Kim, D. *J. Am. Chem. Soc.* **2004**, *126*, 16187.